18TH WORLD CONFERENCE ON EARTHQUAKE ENGINEERING
WCEE2024
MILAN

MILAN, ITALY
30TH JUNE - 5TH JULY 2024

www.wcee2024.it

A NEW APPROACH FOR THE SEISMIC DYNAMICS OF MASONRY STRUCTURES

S. Coccia[1] & M. Como[1]

[1] DICII – University of Rome "Tor Vergata", Via del Politecnico 1, 00133 Rome (Italy)

Abstract: *The aim of this paper is the dynamical collapse analysis of masonry structures affected by sequences of simple pulses of horizontal acceleration. The paper points out the two new aspects that play a fundamental role to define the dynamical collapse of the masonry structures: the critical, or the zero strength, configuration that the structure has to reach just before the collapse, and the accumulation of deformation that takes place in the structure hit by sequences of horizontal acceleration pulses, alternating in sign.*
The collapse of the structure is therefore ruled by the limit critical acceleration ratio between the acceleration intensities A_0 and A_L of the pulse sequences that respectively produce the dynamic and the static collapse and by the effective duration of pulses, pt_0, dilated or contracted compared to the real pulse duration t_0, by means the pulsation p of the motion of the structure.
The paper ends with the determination of the limit static strength λ_{REQ} required in order the structure could sustain, at the limit, the action of a seismic event of the expected acceleration PGA and period T_E.

1. Introduction

The masonry material has a low tensile strength. For this reason, the response of masonry structures cannot ignore their inability to resist tensile stresses. According to the Heyman (1966) no tension model, the masonry structure deforms with mechanisms produced by the alternating opening and closing of cracks (Fig. 1).

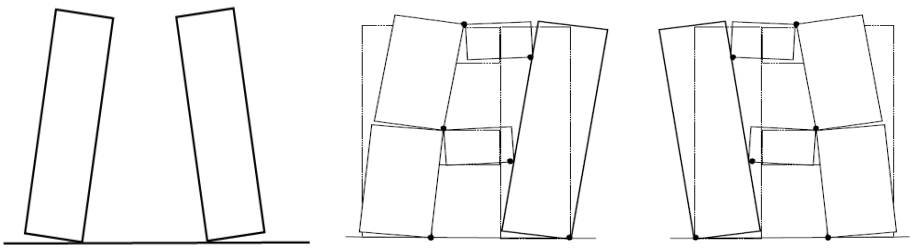

Figure 1. Similar rocking behaviour between the block and the masonry structures.

The rigid block resting on a surface with friction that, during the earthquake shaking, oscillates rotating and detaching alternately, without sliding, from its base section, can thus represent the rocking motion of the masonry structure. Starting from the pioneer work of Housner (1963), who first formulated the motion equation of the rigid block resting over a friction plane, this problem has been investigated in detail, see for example: DeJong and Dimitrakopoulos (2014), Makris and Vassiliou (2013), Mehrotra and DeJong (2020), Prajapati et al. (2022), Voyagaki et al. (2013). Casapulla and others (2010) have written a pioneering paper dealing with the sequence of instantaneous pulses involving resonance effects on rocking motion of a masonry rigid free-standing block. In Coccia et al. (2022), Coccia and Como (2023) and Coccia and Como (under review) the masonry structure is hit by sequences of horizontal acceleration pulses alternating in sign. The authors discover the following two new aspects:

- the way in which the dynamical collapse develops in masonry structures with the reaching of their zero-strength configuration;

- the occurrence of a particular resonance condition that takes place under pulse sequences of particular intensity and wave length: the structure suddenly stops to rock and progressively increases its tilting deformation until the reaching of the zero-strength configuration and the collapse.

These two aspects play a fundamental role in the dynamic collapse of masonry structures – that reveals to be completely different from the static one.

First, at the zero-strength configuration, the weight, the only strength resource of rocking masonry structures, is no longer able to oppose any further increasing of deformation, so that, when, during the motion, this configuration is reached the dynamic collapse must necessarily take place.

Second, under the hammering action of the pulse sequence, the structure gains continuously deformation and is drawn towards the zero-strength configuration. The different geometry existing between the initial and the final critical configurations, gives rise to a continuous change of the position of the mechanism hinges and, consequentially, to a continuous variation of the motion of the structure, as far as to the collapse. A nonlinear analysis of this motion is therefore required.

Two quantities characterize this motion. The first is the limit critical acceleration ratio $q_{0N}= A_{0N}/A_L$ - between the acceleration intensities A_{0N} and A_L of the N pulse sequence that respectively produce the dynamical and the static collapse. The second is the effective duration of pulses, pt_0, dilated or contracted compared to the real pulse duration t_0, by means of the pulsation p, a quantity that distinguishes the structure's motion.

The limit critical acceleration ratios q_{0N} of sequences get closer and closer by increasing the pulse number N of the sequences so that the limit asymptotic curve C_0* can be drawn. This curve provides the asymptotic limit critical acceleration ratio q_0* of sequences of any pulse number and of the chosen pulse duration pt_0. Concluding, the limit static strength λ_{REQ} - required in order the structure could sustain, at the limit, the action of a seismic event of the expected acceleration PGA and the period T_E - is given.

2. Schematization of the seismic input

A typical seismic shaking is composed of a sequence of shocks made up of horizontal and vertical acceleration pulses that follow one after the other with different intensities.

As an example, Fig. 2 shows the most significant part of an accelerogram recorded in Italy, near the city of L'Aquila during the 2009 earthquake, relative to the E-W direction. As can be seen, the maximum value of the horizontal acceleration is equal to 0.67g.

Each shock can be represented by two successive pulses of horizontal acceleration of opposite sign, having an approximately rectangular or sinusoidal trend, of variable intensity and duration. The lowest intensity shocks, present at the beginning and at the end of the accelerogram, are the so-called primary and secondary waves, while the waves included in the central part indicate the arrival of the surface waves, the more severe ones. These last shocks are those that have the longest wavelength: it defines the dominant period T_E of the earthquake (Fig. 2) (Coccia et al, 2022).

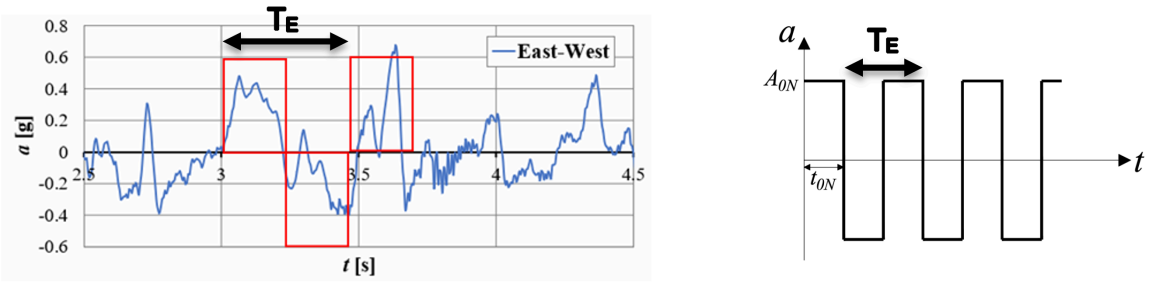

Figure 2. Real and simplified accelerogram.

For the dynamic analysis that follows, the seismic shaking, for simplicity, is assumed to consist of a sequence of alternating rectangular pulses of horizontal acceleration, of the type described in Fig. 2. It approximates the trend of the most severe seismic shocks shown in the same Fig. 2. Only a limited number of shocks characterizes the seismic event. Three quantities define the pulse sequence:

- the number N of pulses,

- the maximum acceleration A_0,

- the duration t_0 of the pulses.

The aim of the research is to analyse the way in which these three quantities are involved in the dynamic collapse of the masonry structures hit by pulse sequences of horizontal accelerations.

3. The motion of the rigid block rocking on a friction plane, the archetype of the masonry structures

According to the results obtained in Coccia et al. (2022), it has been shown that the rigid parallelepiped block, of width B and height H, resting on a plane with friction, can synthetically describe the behaviour of a masonry structure that deforms with mechanisms, due to the incapacity of the material to sustain tensile stresses.

The block, under its weight W, hit by a pulse of horizontal acceleration A, leaves its vertical equilibrium position and starts moving as soon as the line of action of the weight W passes through the corner of the base section of the block (Fig.3).

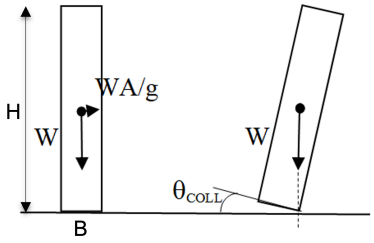

Figure 3. The rigid block

The acceleration of the static collapse of the block is:

$$A_L = g\,B/H \tag{1}$$

From another point of view the acceleration A_L corresponds also to the static collapse multiplier λ_{BL} of the horizontal static load acting on the block:

$$\alpha_{BL} = A_L/g = B/H \tag{2}$$

These results can be extended from the block to the generic masonry structure. In this case A_L will still define the limit static acceleration producing the static collapse of the structure, that is proportional to:

$$\lambda_{STR} = A_L/g \tag{3}$$

i.e., the limit multiplier of static horizontal loads representative of the seismic action, that can be determined via Limit Analysis.

When the horizontal acceleration reaches the value A_L, the motion of the block starts.

Let us now examine this motion of the block under the action of a uniform distribution of horizontal acceleration. The equation governing this motion, for the first time given by Housner (1963), is obtained by the following condition of dynamical equilibrium:

$$\ddot{\theta} I_o = -WR(\alpha_{BL} - \theta) + (WA_0/g)R \tag{4}$$

that, considering that the moment of inertia is given by:

$$I_o = \frac{1}{3}(W/g)4H^2(1+tg^2\alpha_{BL}) \tag{5}$$

gives

$$\ddot{\theta} - p^2\theta = p^2(A_0/g - \alpha_{BL}) \tag{6}$$

with

$$p = \sqrt{\frac{WR}{I_o}} = \sqrt{\frac{3g}{4H\sqrt{1+tg^2\alpha_{BL}}}} \quad (7)$$

the pulsation of the motion and R the distance between the hinge at the base and the centre of gravity of the block.

The block, during its motion can reach, on the other hand, that configuration, called configuration of zero strength or critical configuration, where the resource of strength of the block, due to its weight is lost. This happens if the inclination of the block reaches the rotation θ_{COLL}, as shown in Fig. 3. This rotation is given by:

$$\theta_{COLL} = B/H \quad (8)$$

Eq. (6), by using (8), takes the significant form:

$$\ddot{\theta} - p^2\theta + p^2\theta_{COLL}(1 - A_0/A_L) = 0 \quad (9)$$

This equation, as shown in Coccia and Como (2023) is perfectly analogous to the equation that rules the motion of a generic masonry structure hit by a pulse acceleration if we consider the actual pulsation p of the motion and the actual zero strength rotation θ_{COLL} of the given structure that can be determined, case by case, considering the changes of the mechanism defining the motion of the structure (Coccia and Como, 2023).

4. Extension from the motion of the block to the motion of the generic masonry structure

These considerations extend from the block to the generic masonry structures whose resistance, like that of the block, is due to their weight and geometry. The masonry wall, for instance, as well as the block, swings with non-harmonic oscillations, according to the mechanism produced by the alternating opening and closing of cracks (Fig. 1). All the basic quantities (p, θ_{COLL}, A_L) that define the motion of the block (eq. (9)) must refer to the generic structure.

4.1 The pulsation p of the motion

The pulsation p determines the scaling of the pulse duration of the sequence, that, contracting or dilating the real pulse duration t_0, becomes the effective pulse duration pt_0. This last quantity plays a fundamental role in the seismic dynamics of masonry structures.

Fig. 4 shows, as examples, the variation of the pulsation p versus the no dimensional geometrical characteristics of the structure of:

- a masonry wall, reinforced by a top ring beam and vertical FRP strips, or similar, of length x/H and plated on both sides of the wall, hit by out of plane pulses of horizontal acceleration (Coccia and Como, 2023),

- a circular arch versus the ratio h/Rm for various angles of the opening (Coccia and Como, under review).

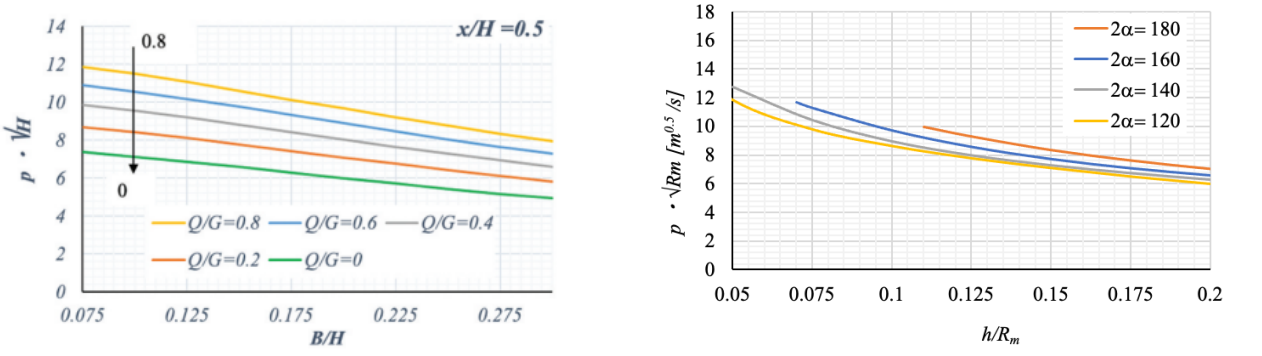

(a) (b)

Figure 4. The pulsation p of: (a): the out of plane motion of the wall, versus the ratio B/H and the length x/H of reinforcing strips and (b): the in-plane motion of the arch, versus h/R_m for various angle of opening

4.2 The configuration of zero strength

The critical (or the zero strength) rotation θ_{COLL} of the block corresponds to the inclination in which the resultant of its weight passes through the centre of rotation at its base. An increase in rotation starting from this configuration causes the weight of the block to go down. The potential energy of the weight in this configuration has reached its maximum. The same happened for any other masonry structure.

A single parameter, the rotation of a single body, defines the geometry of the multibody single degree of freedom mechanism so that we can assume also for the generic masonry structure the critical rotation θ_{COLL} to define the corresponding configuration of zero strength.

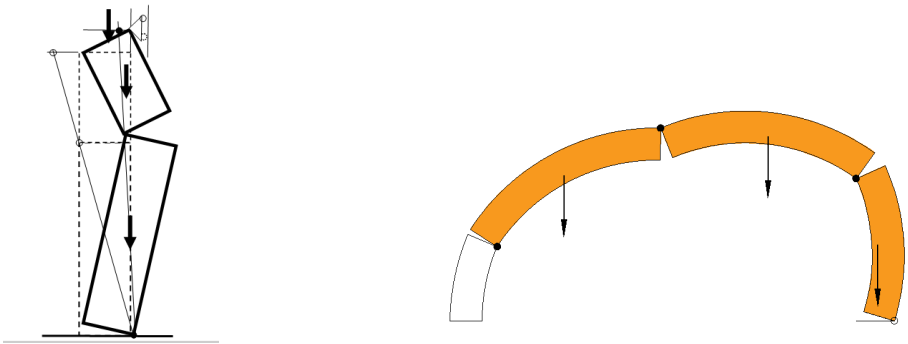

Figure 5. Critical configurations of some examples of masonry structures.

Fig. 5 shows the critical configuration of the wall horizontally fixed at the top, which, under actions orthogonal to its plane, moves with the three-hinged mechanism and that of the masonry arch.

We recognize that in these cases the mechanism changes during motion due to the gradual translation of its internal hinge and reaches the critical configuration when the potential energy of the loads has attained its maximum. The same occurs for the masonry arch of the same Fig.5.

4.3 Deformation build-up under sequence of pulses alternating in sign.

A typical feature that characterizes the seismic dynamics of masonry structures is the accumulation of deformation that develops in them when hit by sequences of acceleration pulses.

Let us consider the case of the rigid masonry structure invested by the sequence S_3 composed by three rectangular pulses alternating in sign, having the acceleration intensity A_{03} and duration t_{03} (Fig.6).

The rotation and the angular velocity of the structure at the end of the first pulse are, according to (9):

$$\begin{aligned} \theta_I(t_{03}) &= \theta_{COLL}(q_{03}-1)(\cosh p\, t_{03}-1) \\ \dot{\theta}_I(t_{03}) &= \theta_{COLL}(q_{03}-1)p \sinh p\, t_{03} \end{aligned} \tag{10}$$

with

$$q_{03} = A_{03}/A_L = A_{03}/(g\lambda_{STR}) \tag{11}$$

is the ratio between the pulse acceleration A_{03} and the static limit A_L (=λ_{STR} g). The rotation of the structure at the end of the first pulse increases both by increasing the acceleration ratio q_{03} and the effective pulse duration pt_{03}.

Let us admit that the zero-strength rotation was not reached at the end of the first pulse so that, taking into account (10) it turns out:

$$(q_{03}-1)(\cosh p\, t_{03}-1) < 1 \tag{12}$$

Let us consider the motion of the block during the action of the second pulse. The equation of the motion is

$$\ddot{\theta}_{II}(\tau) - p^2\theta_{II}(\tau) = -p^2\theta_{COLL}(q_{03}+1) \tag{13}$$

The rotation $\theta_{II}(\tau)$ is connected to the rotation $\theta_I(\tau)$ by means of the conditions:

$$\theta_{II}(0) = \theta_I(t_{03}) \qquad \dot{\theta}_{II}(0) = \dot{\theta}_I(t_{03}) \tag{14}$$

so that the rotation of the structure during the second pulse is

$$\theta_{II}(t) = \left(\dot{\theta}_I(t_{03})/p\right)\sinh p\,t + [\theta_I(t_{03}) - \theta_{COLL}(q_{03}+1)]\cosh p\,t + \theta_{COLL}(q_{03}+1) \tag{15}$$

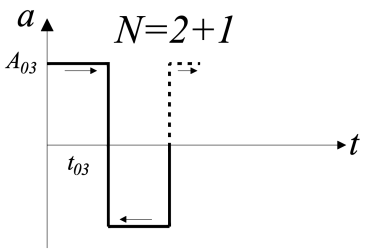

Figure 6. The three-pulse sequence.

The ratio between the rotations $\theta_{II}(t_{03})$ and $\theta_I(t_{03})$, respectively valuated at the end of the second and of the first pulse, considering the (10) and (15), is

$$\psi = \theta_{II}(t_{03})/\theta_I(t_{03}) = 1/\left((q_{03}\text{-}1)(\cosh p\,t_{03}\text{-}1)\right) > 1 \tag{16}$$

Thus, during the action of the second pulse, the rotation of the block *continues to grow* even if the second pulse acts in the opposite direction to the first.

The block, as well as all other masonry structures that deform with mechanisms, accumulate deformation during the sequence. Fig. 7 shows the accumulation of deformation occurring:

- in the rigid block (Coccia, Como, Di Carlo, 2022);

- in the wall of Fig. 5 in an out of plane mechanism (Coccia and Como, 2023);

- in the masonry arch (Coccia and Como, under review).

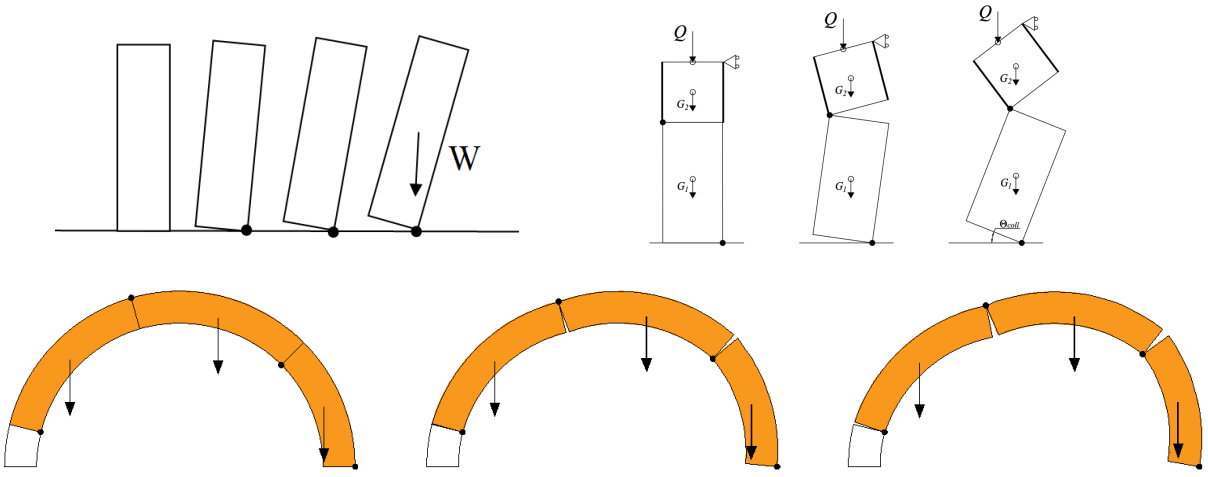

Figure 7. Accumulation of deformation in masonry structures under pulse sequences until reaching the zero-strength configuration.

Fig. 8 reports the most significant results of a numerical investigation developed in (Coccia, Como, Di Carlo, 2022) that confirms the occurrence of the accumulation of rotation in the block hit by actual seismic inputs deduced from real accelerograms. Fig. 8 shows this occurrence of the rotation accumulation in a block, with the assumed height of 6 m, as far as the reaching of the collapse, obtained considering the shorter time intervals where pulses are stronger, of the chosen accelerogram.

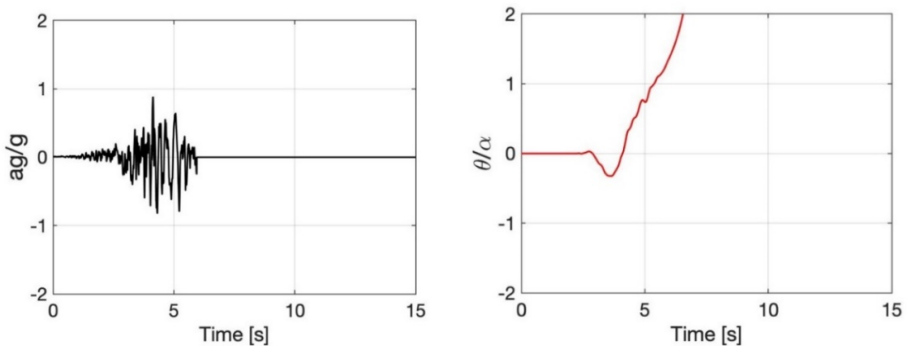

Figure. 8. Accumulation of the rotation in the block.

5. Experimental evidence of the accumulation of deformation in walls hit by pulse sequences.

There is much experimental research on the vibrating table done to analyse the behaviour of masonry walls subject to out of plane seismic actions. On the contrary, there are few researches that, gradually increasing the shaking and intensity, have pushed themselves until they reached the dynamic collapse of the wall. Among the latter we refer to the research of Lönhoff and Sadegh-Azar (2018) in which shaking table tests were made up to reach the collapse of the wall (Fig. 9). The time history of the El Centro Earthquake was used, with peak accelerations of 3.14 m/s^2 reached after 2 sec. The strongest shocks occur in the first 5 seconds. The base acceleration time history was scaled, or increased stepwise, until to reach the failure of the wall. Tests were made to consider the possible influence of the stiffened head of the wall. We make reference to the tests performed without vertical stiffness, indicated as (M20), (M21) and (M22).

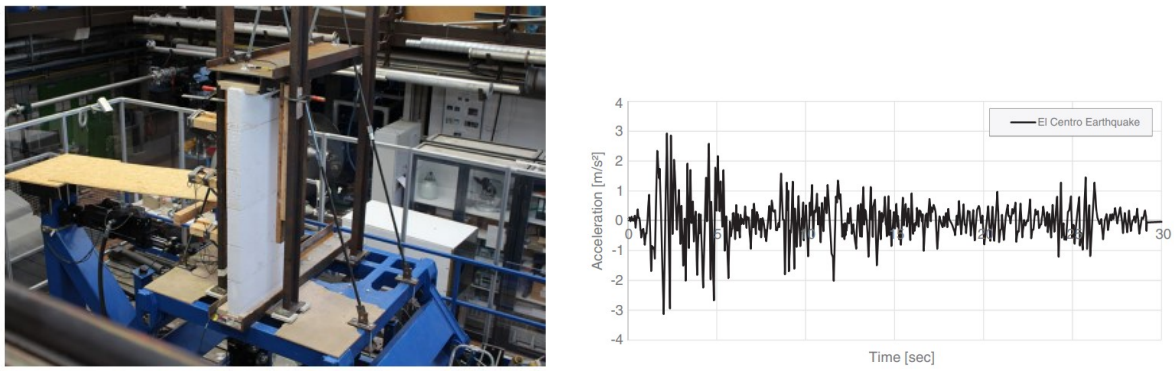

Figure 9. Test set up from Lönhoff and Sadegh-Azar (2018) that used real earthquake time histories.

In the first test (M20), with the time history scaled with a factor of 0.5 the wall, with a rocking motion back and forth, has followed the action of the alternating shocks. The displacements of the wall remained small. The maximum deformation, equal to 1 cm, occurred at the wall centre about in the first 2 secs. In the second test (M21) the motion of M20 was increased up to a scale factor of 0.7. In this case the registered rocking motion of the wall follows still well the shape of the excitation but with a large increase in the deformation. The peak displacement was about 2.5 cm at 2 sec as well as at 5 sec.

In the M22, the excitation of M21 was further increased to a scale factor of 0.95 and the collapse of the wall has been reached. In this last test, the trend of the variation of the displacements of the wall during the time is completely different from the previous one. While in the M20 the motion of the wall substantially reproduces the trend of seismic shocks, in the diagram of Fig. 8 a sudden accumulation of deformation of the wall, reaching about 8 cm, occurs after about 2 secs without any inversion of sign, despite the alternating nature of the violent

shocks. This strong increasing of the displacements occurs uniformly, without any, even small, inversion during the rapid action of the alternating shocks and lasts about 0.5 secs. Immediately after, the wall remains still in the deformed configuration because sustained by the collapse prevention system. The wall can therefore be considered as failed.

Fig. 10a shows the first section of the displacement diagram with the indications, marked by vertical segments, of the times where the ascending part of the diagrams begins or ends.

In Fig. 10b the times are dilated to better show the pulses which follow one another during the ascending phase of the displacements. Four pulses follow each other in this phase, and they are the ones that produce the deformation build up. The first four pulses, indicated in sequence with I, II, III, IV, produce the growth of deformation until, at the end of the fourth pulse, the wall has reached the configuration of zero strength. Consequentially, with the arrival of the fifth pulse, the collapse would have occurred if the wall had not been blocked by the presence of the movement containment system.

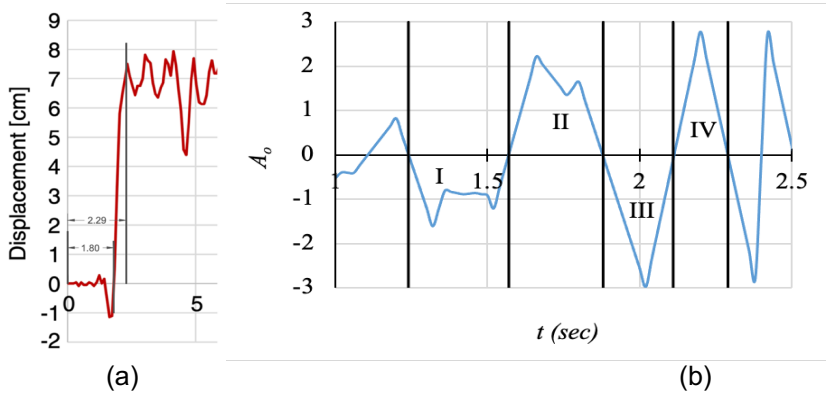

(a) (b)

Figure 10. M22 test in 0-5 sec period (a). Displacement time history; (b) Earthquake time histories [Lönhoff and Sadegh-Azar, 2018].

This result shows that the collapse of the wall takes place with the occurrence of a rotation build up that develops while the shocks, with their hammering action, follow one after the other: it confirms the previsions of our theoretical analysis on the appearance of the deformation accumulation, without inversion of sign, that drags the wall into the configuration of zero strength, just preceding the collapse.

6. Dynamical collapse in the sequence

Let us assume now that the pulses of the sequence S_3 have magnitude A_{03} and duration pt_{03} so that the critical rotation θ_{COLL} is just attained at the end of the second pulse (Fig. 5).

The duration t_{03} of the acceleration pulses of intensity $q_{03}= A_{03}/(g\lambda_{STR})$ required to drag the block into the critical configuration right at the end of the second pulse, is obtained by the following condition:

$$\Theta_{II}(t_{03}) = \left(\dot{\theta}_I(t_{03})/p\right)\sinh p\, t_{03} + [\theta_I(t_{03}) - \theta_{COLL}(q_{03}+1)]\cosh p\, t_{03} + \\ +\theta_{COLL}(q_{03}+1) = \theta_{COLL} \qquad (17)$$

that gives

$$q_{03} = (2\cosh^2 p\, t_{03} - 1)/\left(2\cosh p\, t_{03}(\cosh p\, t_{03} - 1)\right) \qquad (18)$$

The structure, having reached the critical configuration, collapses at the beginning of the third pulse which pushes it to rotate in the same direction beyond the critical angle θ_{COLL}.

Eq. (18), among all the three pulse sequences, provides, for each choice of the effective duration pt_{03} of the pulses, the corresponding limit critical acceleration ratio q_{03} of the three-pulse sequence $S_{03}(pt_{03})$ required to drag the block at the critical configuration just at the end of the second pulse. This sequence is indicated as the *limit critical* three pulse sequence S_{03}.

Conversely, the critical effective duration pt_{03} of the pulses of the critical limit sequence $S_{03}(pt_{03})$ corresponding to the limit critical ratio $q_{03}(t_{03})$ is:

$$pt_{03} = \cosh^{-1}[(2q_{03} - 1)/(2q_{03} - 2)] \quad (19)$$

The rotation of the structure grows as q_{03} grows, so that any three-pulse sequence S'_3 having $q'_3 > q_{03}$ causes the collapse of the element. This sequence is therefore called *critical*, but not limit, as the critical rotation of the structure is reached before the end of the second pulse. Conversely, a sequence with $q''_3 < q_{03}$ is not able to produce the critical rotation at the beginning of the third pulse and does not produce collapse (Fig.11).

Consequentially, the *limit critical ratio* $q_{03} = A_{03}/(g\lambda_{STR})$, defined by (20), is the *smallest acceleration ratio*, among all the critical ratios $q'_3 = A'_{03}/(g\lambda_{STR})$ of the three pulse sequences, having pulses with effective duration pt_{03}, that produce the collapse of the structure. The situation is similar if we consider longer pt'_3 or shorter pt''_3 effective pulse durations.

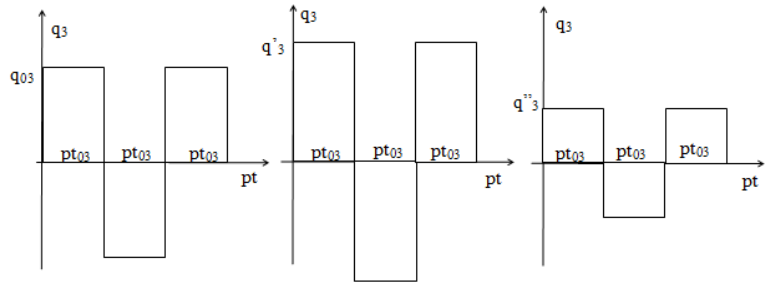

Figure 11. The N=2+1 limit critical sequence, the limit one, and that not producing collapse, obtained by increasing or reducing the acceleration ratio q_{93}

Eq. (18) defines in the plane [pt_{03}, q_{03}] the *critical limit curve* (Fig. 12).

$$C_{03} = [pt_{03}; q_{03}(pt_{03})] \quad (20)$$

that gives, for any value of the effective duration pt_{03} the corresponding value of the limit critical acceleration $q_{03}(pt_{03})$ for the masonry structure.

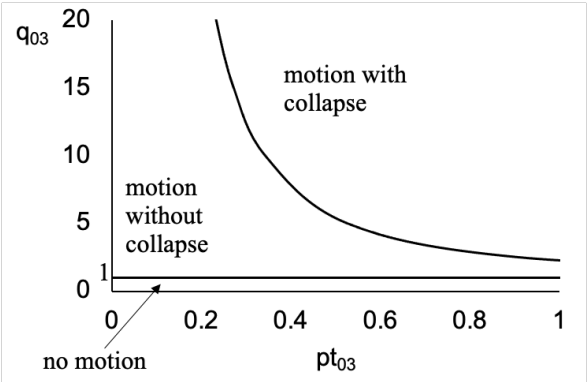

Figure 12. The critical limit curve C_{03}.

7. Sequences of order N. The limit critical asymptotic C_0 of masonry structures

Similarly, the sequences S_N (Fig. 1) are *limit critical* if, for the chosen value of the effective pulse duration pt_{0N} and the critic limit acceleration ratio:

$$q_{0N} = A_{0N}/A_L \quad (21)$$

the block, or the structure, at the end of the penultimate pulse, is dragged into the critical configuration.

In analogy to C_{03}, we can draw in the plane (pt_{0N}; $q_{0N}(pt_{0N})$) the curve C_{0N}:

$$C_{0N}=[pt_{0N};q_{0N}(pt_{0N})] \quad (22)$$

that provides, for any value of the effective duration pt_{0N}, the corresponding value of the limit critical ratio $q_N(pt_{0N})$ of the N pulse sequence that determine the collapse of the structure, just at the beginning of the last pulse of S_N. Fig. 13 shows the limit critical curves C_{03}, C_{05} and C_{07} that correspond to sequences with the pulse number respectively equal to 3, 5 and 7. All the curves give:

$$\lim_{pt_{0N}\to\infty} q_{0N}=1 \quad (23)$$

The C_{0N} collapse limit curves become close to each other and almost overlap when the number N of pulses increases so that the asymptotic critical limit curve C_0^* can be defined.

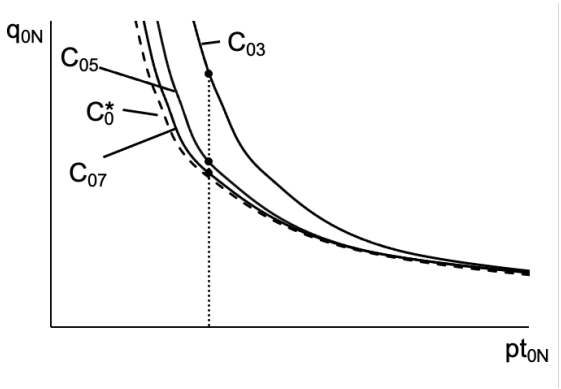

Figure 13. Collapse limit curves

This curve, for any chosen value of the effective pulse duration $pt_0=pT_E/2$, gives the value of *critical limit ratio* q_0^*:

$$q_0^*(pT_E/2) = A_0(pT_E/2)/A_L \quad (24)$$

that is the *minimum* among all the critical values of the acceleration ratios able to lead to collapse the block or the structure. As shown in Coccia and Como (under review), this curve C_0^* can be well represented by the curve C_{07} defined by the equation:

$$q_0^* = q_{07} = (\cosh 6\,pt_0)/(2\cosh p\,t_0(2\cosh 4\,pt_0 + 1)(\cosh p\,t_0 - 1)) \quad (25)$$

Fig. 14 shows the curve C_0^* directly obtained by (27) by assuming $t_0 = T_E/2$ if T_E equals the period of the expected earthquake.

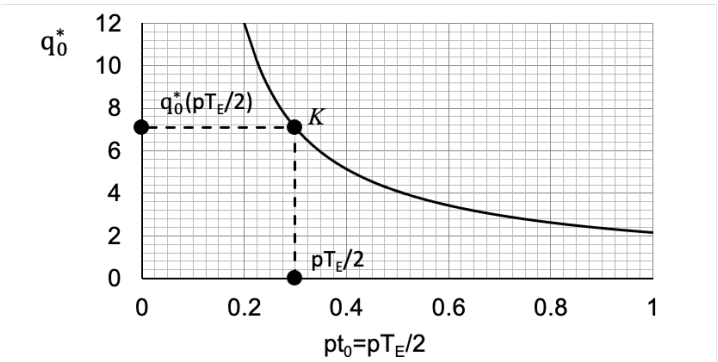

Figure 14. The limit collapse curve C_0^* and the determination of the limit acceleration ratio q_0^* via the specific pulsation pt_0.

8. Safety check of masonry structures in-situ

The proposed seismic verification is based on two quantities that identify the expected earthquake: the PGA, i.e. the maximum horizontal acceleration and the period T_E,. The seismic check is then carried out by evaluating the required horizontal static resistance λ_{REQ} so that the masonry structure, with its pulsation p, could be able to support, at the limit of dynamic collapse, the action of pulse sequences of any order N, having the assigned acceleration intensity PGA and duration TE/2.

The limit collapse curve C_0^* of the column can be used to identify the seismic response of the structure. We fix the point $pT_E/2$ on the abscissa axis pt_0 in the plane (q_0, pt_0) where the collapse limit curve C_0^* is drawn (Fig. 14). The specific duration of the acceleration pulses is defined considering the expected earthquake whose period is T_E. Then we detach the corresponding ordinate:

$$q_0^*(pT_E/2)=[A_0(pT_E/2)/g)]/(\lambda_{STR}) = q_{0k} \quad (26)$$

that intersects the limit curve C_0^* at the point K (Fig. 12). The ordinate K defines the *critical limit ratio* $q_0^*(pT_E/2)$ of the asymptotic sequence of pulses having specific duration $pT_E/2$.

The ratio $q_0^*(pT_E/2) = q_{0K}$, fixed on the ordinate K, for the given seismic strength λ_{STR} (4) , or limit of the structure, gives the *minimum acceleration intensity* A_0/g producing the collapse of the structure among all the sequences, of any order N, of pulses having the effective expected duration $pT_E/2$.

On the contrary, we can obtain the *static horizontal seismic strength* λ_{REQ} *required* for the structure, having pulsation p, could be able to support, at the limit of the collapse, the action of sequences, of any order N, with pulses having the given acceleration intensity $A_0(pT_E/2)$ and duration $T_E/2$.

The value of the required static strength λ_{REQ} of the structure is:

$$\lambda_{REQ} = A_0(pT_E/2)/\left(gq_0^*(pT_E/2)\right) = A_0(pT_E/2)/(gq_{0k}) \quad (27)$$

We remark that q_{0K} is the minimum *acceleration ratio* among all the sequences, of any order N, of pulses having the expected effective duration $pT_E/2$. Consequentially λ_{REQ} represents the *maximum static horizontal seismic strength* that the structure must present to sustain at the limit of the collapse, the action of sequences of any order N, with pulses having the given acceleration intensity $A_0(pT_E/2)$ and the duration $T_E/2$.

Let us admit that in the site the maximum expected acceleration is A_0/g = PGA. Then

$$\lambda_{REQ} = PGA/(gq_{0k}) \quad (28)$$

is the *maximum static horizontal seismic strength required* so that the structure can sustain, at the limit, pulse sequences of any order N, having the expected acceleration intensity PGA and the expected specific duration pT_E /2.

Let us admit that in the site, the maximum expected acceleration is A_0/g = PGA. Then

$$\lambda_{REQ}(q_{0k}) = PGA/(gq_{0k}) > \lambda_{REQ} = PGA/(gq_{0N}) \qquad \forall N \quad (29)$$

Concluding, $\lambda_{REQ}(q_{0k})$ gives the *maximum static horizontal seismic strength required* to the structure to sustain, at the limit, pulse sequences of any order N, having the expected acceleration intensity PGA and the expected specific duration $pT_E/2$.

The static strength λ_{STR} of the structure must be not lower than the required λ_{REQ}, i.e.

$$\lambda_{STR} \geq \lambda_{REQ} \quad (30)$$

Introducing the safety factor $S_0 > 1$ we should better have

$$\lambda_{STR} \geq S_0\lambda_{REQ} \quad (31)$$

The safety level is inferred from $S_0 = 1.5$ calculated through eq. (31).

9. Conclusion

The paper has developed dynamical collapse analysis of masonry structures affected by sequences of simple pulses of horizontal acceleration. The paper points out the two new aspects that play a fundamental role to define the dynamical collapse of the masonry structures: the critical, or the zero strength, configuration that the structure has to reach just before the collapse, and the accumulation of deformation that takes place in the structure hit by sequences of horizontal acceleration pulses, alternating in sign.

The collapse of the structure is ruled by the limit critical acceleration ratio between the acceleration intensities A_0 and A_L of the pulse sequences that respectively produce the dynamic and the static collapse and by the effective duration of pulses, pt_0, dilated or contracted compared to the real pulse duration t_0, by means the pulsation *p* of the motion of the structure.

10. References

Casapulla C., Jossa P., Maione A. (2010). Rocking motion of a masonry rigid block under seismic actions: A new strategy based on the progressive correction of the resonance response. *Ingegneria Sismica*, 27(4), 35 – 48.

Coccia, S., and Como, M. (2023). Out-of-Plane Dynamical Strength of Masonry Walls Under Seismic Actions. *Journal of Earthquake Engineering*, 1-29.

Coccia, S., Como, M., and Di Carlo, F. (2022). The Slender Rigid Block: Archetype for the Seismic Analysis of Masonry Structures. *Journal of Earthquake Engineering*, 1-25.

Coccia, S., and Como, M. (2023). Dynamic collapse of masonry arches. *Journal of Earthquake Engineering*, under review.

DeJong, M. J., and Dimitrakopoulos, E. G. (2014). Dynamically equivalent rocking structures. *Earthquake engineering & structural dynamics*, 43(10), 1543-1563.

Heyman, J. (1966). The stone skeleton. *International Journal of solids and structures*, *2*(2), 249-279.

Housner, G. W. (1963). The behavior of inverted pendulum structures during earthquakes. *Bulletin of the seismological society of America*, 53(2), 403-417.

Lönhoff, M., & Sadegh-Azar, H. (2018). Seismic out-of-plane behavior of unreinforced masonry walls. *ce/papers*, *2*(4), 291-299.

Makris, N., and M. F. Vassiliou. 2013. Planar rocking response and stability analysis of an array of free-standing columns capped with a freely supported rigid beam. Earthquake Engineering and Structural Dynamics 42 (3):431–49.

Mehrotra, A., and M. J. DeJong. 2020. A methodology to account for interface flexibility and crushing effects in multi-block masonry collapse mechanisms. Meccanica 55 (6):1237–61.

Prajapati, S., G. Destro Bisol, O. AlShawa, and L. Sorrentino. 2022. Non-linear dynamic model of a two-bodies vertical spanning wall elastically restrained at the top. Earthquake Engineering & Structural Dynamics 51 (11):2627–47.

Voyagaki, E., I. N. Psycharis, and G. Mylonakis. 2013. Rocking response and overturning criteria for free standing rigid blocks to single-lobe pulses. Soil Dynamics and Earthquake Engineering 46:85–95. doi:10.1016/j. soil dyn.2012.11.010.